IEEE Photonics Journal
An IEEE Photonics Society Publication

Open Access

Multiuser MIMO-OFDM for Visible Light Communications

Volume 7, Number 6, December 2015

Qi Wang, Student Member, IEEE
Zhaocheng Wang, Senior Member, IEEE
Linglong Dai, Senior Member, IEEE

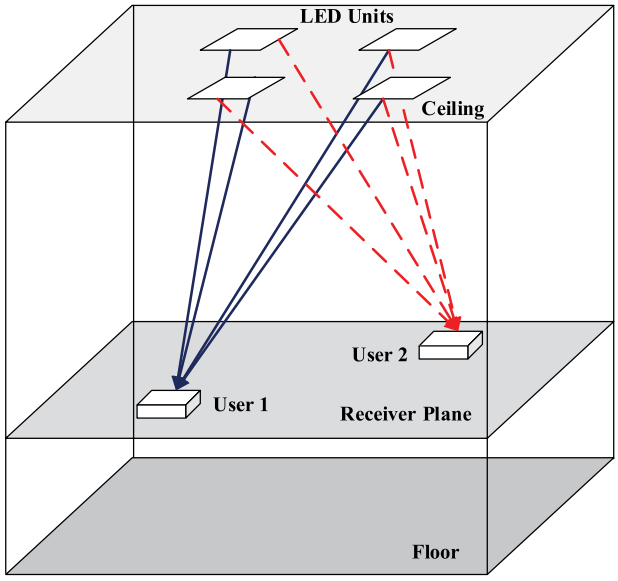

DOI: 10.1109/JPHOT.2015.2497224
1943-0655 © 2015 IEEE

IEEE photonics SOCIETY

IEEE

Multiuser MIMO-OFDM for Visible Light Communications

Qi Wang, *Student Member, IEEE*, Zhaocheng Wang, *Senior Member, IEEE*, and Linglong Dai, *Senior Member, IEEE*

Department of Electronic Engineering, Tsinghua National Laboratory for Information Science and Technology (TNList), Tsinghua University, Beijing 100084, China

DOI: 10.1109/JPHOT.2015.2497224

Manuscript received August 26, 2015; revised October 20, 2015; accepted October 29, 2015. Date of publication November 2, 2015; date of current version November 10, 2015. This work was supported in part by the National Key Basic Research Program of China under Grant 2013CB329203, by the National Nature Science Foundation of China under Grant 61271266, by the Shenzhen Visible Light Communication System Key Laboratory under Grant ZDSYS20140512114229398, by the Shenzhen Wireless over Visible Light Communication Technology Engineering Laboratory under Grant SDRC [2012] No.1440, and by the Shenzhen Peacock Plan under Grant 1108170036003286. Corresponding author: Z. Wang (e-mail: zcwang@tsinghua.edu.cn).

Abstract: Visible light communication (VLC) is emerging as a promising technique to provide ubiquitous wireless connection. In this paper, a multiuser VLC system utilizing multiple-input multiple-output (MIMO) orthogonal frequency-division multiplexing (OFDM) is investigated. Since the distances of the multiple transmitter–receiver links are different, their temporal delays are also different, resulting in complex channel gain and phase differences when transformed to the frequency domain. For each subcarrier in OFDM, the corresponding precoding matrix is calculated in the frequency domain to eliminate multiuser interference. Phase information in the frequency domain is first considered, where complex, instead of real, channel matrices are used for precoding, which reduces the channel correlation and achieves better performance. Moreover, minimum dc bias, unified dc bias, and asymmetrically clipped optical OFDM-based schemes are proposed to generate real-valued nonnegative signals for intensity modulation, and their performances are validated via simulations with zero forcing and minimum mean-squared error (MMSE) precoding techniques.

Index Terms: Visible light communication (VLC), multiple-input multiple-output (MIMO), orthogonal frequency-division multiplexing (OFDM), multiuser, precoding.

1. Introduction

In recent years, visible light communication (VLC) has attracted increasing attention from both academia and industry since it has many advantages, such as wide unregulated bandwidth, high security, and low cost [1], [2]. It has been considered as a promising complementary technique to traditional radio frequency (RF) communications in fifth-generation (5G) and beyond wireless communications, especially in indoor applications [3], [4]. In indoor VLC systems, light-emitting diodes (LEDs) for illumination are used for data transmission at the same time, which is energy efficient. For low cost implementation, VLC systems typically utilize intensity modulation with direct detection (IM/DD), where the information is conveyed through the intensity of LEDs and detected by photodiodes (PDs) at the receiver.

Despite the fact that visible light spectrum is as wide as several terahertz, the bandwidth of off-the-shelf LED is limited, which makes it very challenging to achieve high data rate transmission [5]. Meanwhile, in order to provide sufficient illumination, multiple LED units are usually installed in a single room [6]. Therefore, multiple-input multiple-output (MIMO) techniques can be naturally employed in indoor VLC systems to boost the data rate, and various optical MIMO techniques have been investigated in [7]. Recently, multiuser MIMO (MU-MIMO) has been studied for VLC systems and several precoding schemes have been proposed, which are different from conventional RF systems since only real-valued nonnegative signals can be transmitted [8]–[11]. In [8], the performances of zero forcing and dirty paper coding schemes are compared for indoor VLC broadcasting system. An optimal linear precoding transmitter is derived based on the minimum mean-squared error (MMSE) criterion in [9], while block diagonalization precoding algorithm is investigated in [10]. However, indoor VLC channels are typically highly correlated since there is no phase information and line-of-sight (LOS) scenario is mostly considered, which is unfavorable for the application of MIMO techniques and degrades the performance [12]. As a spectrally efficient modulation approach, optical orthogonal frequency-division multiplexing (OFDM) is intensively utilized in VLC systems and up to Gbps point-to-point data transmissions have been reported [13]–[17]. MIMO-OFDM is a popular technique in RF systems in order to support multiuser service and provide high data rate transmission [18], [19], however it has rarely been studied in VLC systems. In [20], a MIMO-OFDM VLC system is demonstrated, but it requires an imaging diversity receiver to distinguish signals from different LEDs, which is infeasible for multiuser scenarios.

In this paper, multiuser MIMO-OFDM (MU-MIMO-OFDM) is investigated for indoor VLC systems. Considering the distances of the multiple transmitter-receiver links are different, their temporal delays are also different, resulting in complex channel gain and phase differences when transformed to the frequency domain. The phase difference can not be neglected when wide-band systems are considered, especially for the subcarriers with high frequencies. Therefore, in our proposed scheme, the precoding matrix is calculated for each subcarrier in OFDM to eliminate multiuser interference. Different from state-of-the-art schemes, complex rather than real channel matrices can be used for precoding, which reduces the channel correlation with one more degree of freedom and improves the system performance. Moreover, in order to generate nonnegative signals for transmission, two different DC bias and scaling schemes, namely, minimum DC bias and unified DC bias, are proposed and compared with the scheme using asymmetrically clipped optical OFDM (ACO-OFDM). Our simulations show that the minimum DC bias scheme achieves higher spectral efficiency, while the unified DC bias scheme provides better illumination performance.

The following notations are used throughout this paper. Lowercase letters denote time-domain signals, e.g., x, whereas the corresponding uppercase letters represent frequency-domain signals, e.g., X. Boldface lowercase letters denote vectors, e.g., $\mathbf{x}$, and boldface uppercase letters represent matrices, e.g., $\mathbf{X}$. $(\cdot)^*$ is the conjugate operator. $(\cdot)^T$ and $(\cdot)^H$ are the transpose and Hermitian transpose operators for vector or matrix. $(\cdot)^\dagger$ and $(\cdot)^{-1}$ are pseudo-inverse and inverse operators for a matrix, respectively. $E(\cdot)$ denotes the expectation operation.

2. System Model

An MU-MIMO VLC system is illustrated in Fig. 1, where a single room is equipped with multiple LED units for illumination, which can cooperate to transmit information for multiple users simultaneously. In this paper, we consider the system with N_t LED units at the ceiling. N_r users each with a single PD are assumed on the same receiving plane for simplicity, which is between the floor and the ceiling of the room, where we have $N_t \geq N_r$. In order to eliminate multiuser interference, the transmitted $N_r \times 1$ data vector $\mathbf{d}$ is first precoded into an $N_t \times 1$ transmitted vector $\mathbf{x}$. Since VLC systems utilizes intensity modulation, the transmitted vector should be real-valued and nonnegative, and DC bias is added to each LED unit.

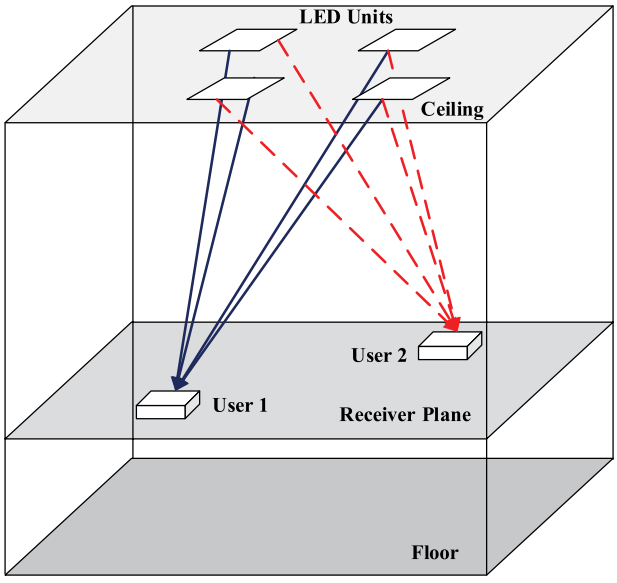

Fig. 1. MU-MIMO VLC system.

The DC gain of the subchannel $h_{p,q}^{\mathrm{DC}}$ between the qth LED unit and the pth user is expressed as [12]

$$h_{p,q}^{\mathrm{DC}} = \begin{cases} \frac{\rho_p A_p}{d_{p,q}^2} R(\phi_q)\cos(\varphi_{p,q}), & \varphi_{p,q} \le \Psi_{c,p} \\ 0, & \varphi_{p,q} > \Psi_{c,p} \end{cases} \tag{1}$$

where ρ_p denotes the responsivity coefficient of the PD, $d_{p,q}$ is the distance between the qth LED unit and the pth user, ϕ_q is the emission angle of the qth LED unit, $\varphi_{p,q}$ is the incidence angle of the light, and $\Psi_{c,p}$ is the receiver field of view (FOV) of the pth user. Unlike conventional RF channels, the channel matrix $\mathbf{H}^{\mathrm{DC}} = \{h_{p,q}^{\mathrm{DC}}\}_{N_r \times N_t}$ is real-valued and commonly highly correlated when the users are located close [7]. For the pth user, the receiver collection area is denoted as A_p, which can be calculated by

$$A_p = \gamma^2 A_{\mathrm{PD},p} / \sin(\Psi_{c,p}) \tag{2}$$

where γ is the concentrator refractive index of the PD, $A_{\mathrm{PD},p}$ is the PD area of the pth user. In (1), $R(\phi_{p,q})$ denotes the generalized Lambertian radiant intensity given by [12]

$$R(\phi_q) = \big((m+1)\cos^m(\phi_q)\big)/2\pi \tag{3}$$

where m is the order of Lambertian emission.

At the receiver of each user, the optical signal is directly detected by the corresponding PD, which generates an electric signal proportional to the received optical power. Besides that, shot noise and thermal noise are induced at the receiver, which can be modeled as real-valued additive white Gaussian noise (AWGN) with zero mean, and the variance of the noise at the pth user can be written as [12]

$$\sigma_p^2 = 2eP_pB + 2e\rho_p\chi_{\mathrm{amb}}A_p\big(1-\cos(\Psi_{c,p})\big)B + i_{\mathrm{amp}}^2 \tag{4}$$

where e is the electronic charge, χ_{amb} is the ambient light photocurrent, B is the bandwidth of receiver, and i_{amp} is the preamplifier noise current density. P_p is the average received optical power at the pth user collected from all the LED units.

3. MU-MIMO-OFDM for VLC System

In existing MU-MIMO VLC systems, single-carrier modulations are utilized with limited bandwidth [8]–[10]. Therefore, precoding is conducted in the time domain and only the DC channel gain in (1) is considered. Since the distances of the multiple transmitter-receiver links are different, their temporal delays are also different, resulting in complex channel gain and phase differences when transformed to the frequency domain. The time-domain channel response from the qth LED unit to the pth user in (1) can be rewritten as

$$h_{p,q}(t) = h_{p,q}^{\mathrm{DC}}\delta\left(t - \frac{d_{p,q}}{c}\right) \tag{5}$$

where $\delta(\cdot)$ denotes the Dirac delta function and c is the speed of light. Correspondingly, the frequency-domain channel response for the kth subcarrier is given by

$$H_{p,q,k} = h_{p,q}^{\mathrm{DC}}\exp\left(-\frac{j2\pi kBd_{p,q}}{Nc}\right) \tag{6}$$

where B denotes the system bandwidth, and N is the size of fast Fourier transform (FFT). j is the imaginary unit, and $j = \sqrt{-1}$. It can be seen that the phase of the frequency-domain channel gain is proportional to the bandwidth. Moreover, when the temporal delay is considered, the frequency-domain channel response is complex-valued, which provides an extra dimension and reduces the channel correlation with the phase differences of multiple links. However, in order to achieve up to 100 Gbps high data rate transmission [21]–[23], wide bandwidth optical components are used, and the phase in the complex channel gain can not be neglected anymore. Therefore, MU-MIMO-OFDM scheme is proposed for VLC system and precoding is performed on different frequencies individually.

We consider a MU-MIMO-OFDM VLC system with the bandwidth of B, which is divided into N subcarriers in OFDM frames. For the pth user, the information bit stream is firstly mapped onto the complex-valued symbols $D_{p,k}$, $k = 0,\ 1, \ldots,\ N-1$, according to the chosen constellations, such as phase shift keying (PSK) or quadrature amplitude modulation (QAM). Since intensity modulation requires real-valued output, Hermitian symmetry should be imposed on the OFDM subcarriers where we have $D_{p,k} = D_{p,N-k}^{*}$, $k = 1, 2, \ldots,\ N/2-1$, and the subcarriers $D_{p,0}$ and $D_{p,N/2}$ are set to zero.

At the transmitter of MU-MIMO-OFDM VLC system, precoding is performed on each subcarrier to eliminate multiuser interference. We denote the precoding weights for the kth $(k = 0, 1, \ldots, N-1)$ subcarrier as $\{W_{p,q,k},\ 1 \le p \le N_r,\ 1 \le q \le N_t\}$, which can be complex-valued. By adding up all the weighted symbols from N_r users at the qth LED unit, the frequency-domain signal can be written as

$$X_{q,k} = \sum_{p=1}^{N_r} W_{p,q,k}D_{p,k}, \qquad k = 0, 1, \ldots, N-1 \tag{7}$$

which is also complex-valued.

Afterwards, the frequency-domain signals for the qth LED unit are converted to the time domain by inverse fast Fourier transform (IFFT) as

$$x_{q,n} = \frac{1}{\sqrt{N}}\sum_{k=0}^{N-1} X_{q,n}\exp\left(j\frac{2\pi}{N}nk\right), \qquad n = 0, 1, \ldots, N-1 \tag{8}$$

which are real-valued since the subcarriers satisfy Hermitian symmetry.

At the beginning of each time-domain OFDM symbol $\mathbf{x}_q = [x_{q,0}, x_{q,1}, \ldots, x_{q,N-1}]^T$, a cyclic prefix (CP) is added to eliminate the inter-symbol interference at the receiver. Since $x_{q,n}$ in (8) may be

negative in some points, a DC bias $P_{\mathrm{DC},q}$ needs to be added to the qth transmitter to obtain non-negative signals for emission, which is called DC-biased optical OFDM (DCO-OFDM).

3.1. Precoder Design

At the receiver of the pth user, FFT is performed on the received signals to generate frequency-domain symbols given by

$$\begin{aligned} R_{p,k} &= \sum_{q=1}^{N_t} H_{p,q,k} X_{q,k} + Z_{p,k} \\ &= \mathbf{H}_{p,k}^T \mathbf{W}_{p,k} D_{p,k} + \sum_{l \neq p}^{N_t} \mathbf{H}_{l,k}^T \mathbf{W}_{l,k} D_{l,k} + Z_{p,k}, \qquad k = 0, 1, \ldots, N-1 \end{aligned} \tag{9}$$

where $\mathbf{H}_{p,k}^T$, $\mathbf{W}_{p,k}$, and $\mathbf{W}_{l,k}$ are $N_t \times 1$ vectors of channel gain and precoding weights for the kth subcarrier; and $Z_{p,k}$ denotes the equivalent noise on the kth subcarrier. The first term $\mathbf{H}_{p,k}^T \mathbf{W}_{p,k} D_{p,k}$ in (9) denotes the desired signal for the pth user, while the second term $\sum_{l \neq p}^{N_t} \mathbf{H}_{l,k}^T \mathbf{W}_{l,k} D_{l,k}$ is the inter-user interference to the pth user, which should be eliminated by precoding.

When all the N_r users are considered, we can rewrite (9) in the matrix form as

$$\mathbf{R}_k = \mathbf{H}_k \mathbf{W}_k \mathbf{D}_k + \mathbf{Z}_k, \qquad k = 0, 1, \ldots, N-1 \tag{10}$$

where $\mathbf{D}_k = [D_{1,k}, D_{2,k}, \ldots, D_{N_r,k}]^T$ and $\mathbf{R}_k = [R_{1,k}, R_{2,k}, \ldots, R_{N_r,k}]^T$ denote the transmitted and received symbol vectors on the kth subcarrier, $\mathbf{H}_k = [\mathbf{H}_{1,k}, \mathbf{H}_{2,k}, \ldots, \mathbf{H}_{N_r,k}]^T$ and $\mathbf{W}_k = [\mathbf{W}_{1,k}, \mathbf{W}_{2,k}, \ldots, \mathbf{W}_{N_r,k}]$ represent the corresponding channel and precoding matrices, $\mathbf{Z}_k$ is the noise vector on the kth subcarrier.

As we can see in (6), the channel matrices for different subcarriers are different due to temporal delays, their corresponding precoding matrices should be calculated separately. Several precoding schemes have been proposed for MU-MIMO in RF systems [24], [25]. In particular, we use two well-known techniques to eliminate the inter-user interference, namely, zero forcing and MMSE algorithms.

A simple way to deal with inter-user interference is zero forcing, which eliminates the interference by directly forcing the interference terms to be zeros, i.e., the matrix $\mathbf{H}_k \mathbf{W}_k$ is forced to be diagonal as [24]

$$\mathbf{H}_k \mathbf{W}_k = \mathrm{diag}(\boldsymbol{\lambda}_k) \tag{11}$$

where all the elements in $\boldsymbol{\lambda}_k$ are positive, and the precoding matrix can be calculated by

$$\mathbf{W}_k = \mathbf{H}_k^{\dagger} \mathrm{diag}(\boldsymbol{\lambda}_k) = \mathbf{H}_k^H \left(\mathbf{H}_k \mathbf{H}_k^H\right)^{-1} \mathrm{diag}(\boldsymbol{\lambda}_k). \tag{12}$$

Zero forcing is a good precoding approach for high power or low noise scenarios. However, when the channel matrix is ill-conditioned, zero forcing requires a large normalization factor, which will dramatically reduce the received power [25]. Therefore, when the signal-to-noise ratio (SNR) at the receiver is low, zero forcing can not achieve a good performance since noise instead of interference is the dominant impairment of the system.

In linear MMSE precoding, however, the interference at the receivers is not identically zero, which achieves a tradeoff between interference and noise based on which one is the dominant part in the signal-to-interference-plus-noise ratio (SINR) at the receiver. The MMSE-based precoding matrix is given by [25]

$$\mathbf{W}_k = \mathbf{H}_k^H \left(\mathbf{H}_k \mathbf{H}_k^H + \mathrm{diag}\left(\sigma_{\mathbf{Z}_k}^2\right)\right)^{-1} \mathrm{diag}(\boldsymbol{\lambda}_k) \tag{13}$$

where $\sigma_{\mathbf{Z}_k}^2$ denotes the variance vector of $\mathbf{Z}_k$.

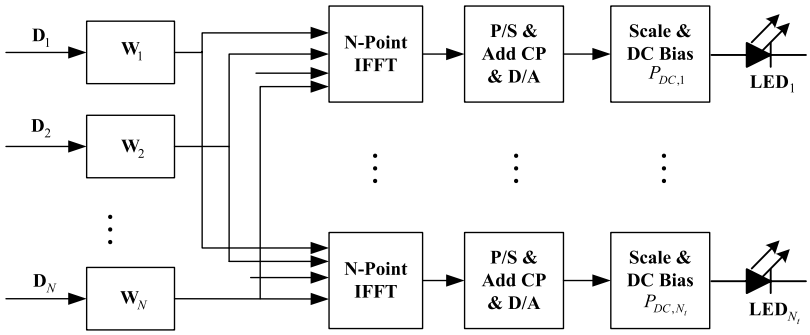

Fig. 2. MU-MIMO-OFDM VLC system with N_r users, N_t LED units, and N subcarriers.

3.2. DCO-OFDM-Based MU-MIMO VLC

Since the generated OFDM time-domain signal $x_{q,n}$ by (8) is bipolar, DC bias should be added to each transmitter to obtain non-negative signals for emission, which is denoted as $P_{\mathrm{DC},q}$ for the qth transmitter. The diagram of the proposed system is illustrated in Fig. 2. According to the central limit theorem, $x_{q,n}$ approximates a Gaussian distribution when $N \geq 64$, and it might have a very large absolute value [15]. Therefore, a DC bias can not necessarily guarantee that all the signals become non-negative and part of the signals should be clipped, leading to undesired clipping distortion. The DC bias for the qth transmitter can be written as [26]

$$\bar{P}_{\mathrm{DC},q} = \eta \sqrt{E\left\{x_{q,n}^2\right\}} \tag{14}$$

which is usually denoted in the form of $10\log_{10}(\eta^2+1)$, dB since it represents the increase in electric power of original OFDM signals, where η represents the DC bias ratio. When we use a larger DC bias, there will be less signals clipped, resulting in smaller clipping distortion. However, it is inefficient in terms of power since DC bias does not carry information. There should be a tradeoff between the DC bias and clipping distortion, and we can define a minimum DC bias ratio η_0 to avoid clipping distortion [26].

When precoding is applied at the transmitter, the electric power of the N_t transmitters is different, which requires different minimum DC bias. If we employ different minimum DC biases for different LED units, we have

$$\bar{P}_{\mathrm{DC},q} = \eta_0 \sqrt{E\left\{x_{q,n}^2\right\}}, \qquad q = 0, 1, \ldots, N_t - 1 \tag{15}$$

which is denoted as the *minimum DC bias scheme*, and the emitted optical power of the qth LED unit is given by

$$P_{\mathrm{opt},q} = E\{x_{q,n} + \bar{P}_{\mathrm{DC},q}\} = E\{x_{q,n}\} + \bar{P}_{\mathrm{DC},q} = \bar{P}_{\mathrm{DC},q} \tag{16}$$

where the equality holds since the expectation of $x_{q,n}$ is zero according to (8).

When the average optical power of all the LED units is constrained to P for illumination requirement, the biased signal should be scaled and the transmitted signal for the qth LED unit is written as

$$y_{q,n} = \alpha(x_{q,n} + \bar{P}_{\mathrm{DC},q}) \tag{17}$$

where the scaling factor can be calculated as

$$\alpha = \frac{N_t P}{\sum_{q=1}^{N_t} \bar{P}_{\mathrm{DC},q}} = \frac{N_t P}{\eta_0 \sum_{q=1}^{N_t} \sqrt{E\left\{x_{q,n}^2\right\}}}. \tag{18}$$

Therefore, the actual DC bias for the qth LED unit is given by

$$P_{\mathrm{DC},q} = \alpha \bar{P}_{\mathrm{DC},q} = \frac{\sqrt{E\left\{x_{q,n}^2\right\}} N_t P}{\sum_{q=1}^{N_t} \sqrt{E\left\{x_{q,n}^2\right\}}}, \qquad q = 0, 1, \ldots, N_t - 1. \tag{19}$$

Since it can be seen in (19) that the emitted optical power for the N_t LED units is different and it will change when the users move on the receiver plane, which will affect the illumination performance of LEDs. In order to provide data transmission and high quality illumination at the same time, we consider a *unified DC bias scheme*, where all the LED units use the same DC bias as

$$P_{\mathrm{DC},q} = P. \tag{20}$$

However, in order to avoid clipping distortion at all the N_t transmitters, this DC bias should satisfy requirement of the transmitter with maximum electric power, and the corresponding scaling factor is given by

$$\alpha = \frac{P}{\eta_0 \sqrt{\max\limits_{1 \leqslant q \leqslant N_t} \left(E\left\{x_{q,n}^2\right\} \right)}}. \tag{21}$$

Since larger DC biases are utilized for most of the LED units without maximum electric power, the power efficiency of the system is reduced accordingly.

3.3. ACO-OFDM-Based MU-MIMO VLC

Alternatively, a power-efficient optical OFDM scheme can be utilized to avoid DC bias, namely, ACO-OFDM [27]. In ACO-OFDM, only the odd subcarriers are modulated to carry useful information, while the even subcarriers are set to zero. In this way, the time-domain signals of ACO-OFDM are antisymmetric, where we have

$$x_{q,n} = -x_{q,n+N/2}, \qquad n = 0, 1, \ldots, N - 1. \tag{22}$$

It has been proved in [27] that the time-domain signals can be clipped at zero without information loss. At the receiver, the symbols on the odd subcarriers can be directly detected by FFT since the clipping distortion only falls on the even subcarriers. However, scaling is still required to fulfill the illumination requirement of P. Since $x_{q,n}$ follows a Gaussian distribution when $N \geq 64$, the optical power of the clipped ACO-OFDM signals $x_{q,n}^{(c)}$ can be given by [17], [26]

$$P_{\mathrm{opt},q} = E\left\{x_{q,n}^{(c)}\right\} = \sqrt{E\left\{x_{q,n}^2\right\}/2\pi} \tag{23}$$

and the scaling factor for the qth LED unit is calculated by

$$\alpha = \frac{N_t P}{\sum_{q=1}^{N_t} P_{\mathrm{opt},q}} = \frac{N_t P}{\sum_{q=1}^{N_t} \sqrt{E\left\{x_{q,n}^2\right\}/2\pi}}. \tag{24}$$

Since no DC bias is required in ACO-OFDM, it is more power efficient compared with the scheme with DC bias. When the same optical power is given, ACO-OFDM-based scheme can use higher-order modulations to increase the spectral efficiency. However, only the odd subcarriers are unoccupied in ACO-OFDM, which conversely reduces the spectral efficiency by half when the same modulation order are used. Therefore, the disuse of DC bias can not guarantee the improvement of spectral efficiency, which will be demonstrated by simulations.

TABLE 1

Simulation parameters for VLC system configuration

Room size (length × width × height)	5 m × 5 m × 3 m
LED 1 coordinate	[1.25 1.25 3]
LED 2 coordinate	[1.25 3.75 3]
LED 3 coordinate	[3.75 1.25 3]
LED 4 coordinate	[3.75 3.75 3]
LED emission angle ϕ_q	60 deg
PD area $A_{PD,p}$	1 cm^2
PD responsivity coefficient ρ_p	0.4 A/W
PD concentrator refractive index γ	1.5
Lambertian emission mode number m	1
Receiver FOV angle $\Psi_{c,p}$	62 deg
Pre-amplifier noise density i_{amp}	5 pA/Hz$^{-1/2}$
Ambient light photocurrent χ_{amp}	10.93 A/m^2/Sr
System bandwidth B	1 GHz
OFDM subcarrier number N	64
Cyclic prefix length N_{CP}	3

4. Simulation Results

The performance of the MU-MIMO-OFDM VLC is validated via simulations with 4 LED units and two users in terms of the aggregate achievable spectral efficiency, which is calculated with all the SINRs at the receiver by $\sum_{p=1}^{N_r} \log_2(1 + \text{SINR}_p)$. The simulation parameters are listed in Table 1. The parameters for LEDs and PDs are chosen from [12]. Since the vertical distance between the ceiling and the receiver plane is 2.15 m, the horizontal distance between the LED and receiver can be as large as $2.15 \cdot \tan(62^\circ)$ m ≈ 4.04 m, which is large enough to cover the entire room. In most occasions, the user can receive information from four LEDs. Even if the user is at the corner of the room, it can still receive information from three LEDs. Two cases of users' locations are considered. In Case 1, the user 1's coordinate is [2.5 2.5 0.85], which is in the center of the room, while user 2's coordinate is [3.2 3.9 0.85]. It is a relatively good scenario since the two users are separated far enough, thus having a uncorrelated channel matrix. In Case 2, the two users' coordinates are [2.05 1.6 0.85] and [2.05 1.4 0.85], which are very close and their corresponding channel matrix is ill-conditioned. Zero forcing and MMSE precoding schemes are used for both cases. The minimum DC bias factor η_0 is set to 3 so that less than 0.15% signals would be clipped at the transmitter and the clipping distortion is negligible.

Fig. 3 depicts the spectral efficiency of each subcarrier in OFDM with the average emitted optical power $P = 1$ Watt (0 dBW expressed by decibel Watt), where DCO-OFDM is utilized with minimum DC bias for each transmitter. Since Hermitian symmetry is applied, only the first to 31th subcarriers carry useful information. It can be seen that when the subcarrier index increases, the spectral efficiency improves, especially in Case 2. This is because the subcarrier with higher index has more phase difference, which makes the channel matrix more uncorrelated, and this improvement is more useful for correlated scenario, as in Case 2.

Fig. 4 shows the average spectral efficiency with different average emitted optical power, where DCO-OFDM is utilized with minimum DC bias and unified DC bias according to Section 3.2. It can be seen that MMSE outperforms zero forcing in both cases. MMSE achieves more spectral efficiency when the optical power is low and the noise is the dominant part of interference-plus-noise. The performance gain of MMSE becomes larger in Case 2 since its channel matrix is more ill-conditioned. Besides that, the system with minimum DC bias according to (15) and (18) achieves more spectral efficiency than that with unified DC bias according to (19) and (20) since more power are used for data transmission. However, the system with unified DC bias provides better illumination performance.

The performance comparison of ACO-OFDM-based and DCO-OFDM-based schemes is illustrated in Fig. 5, where DCO-OFDM employs the minimum DC bias for each transmitter and zero

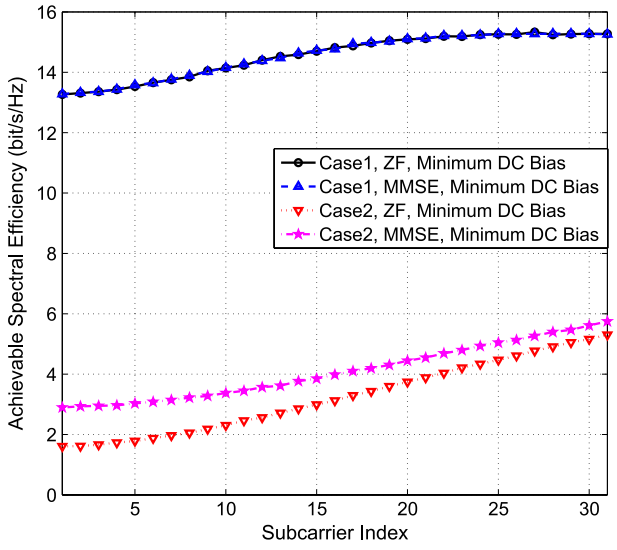

Fig. 3. Spectral efficiency with minimum DC bias and the average emitted optical power $P = 0$ dB.

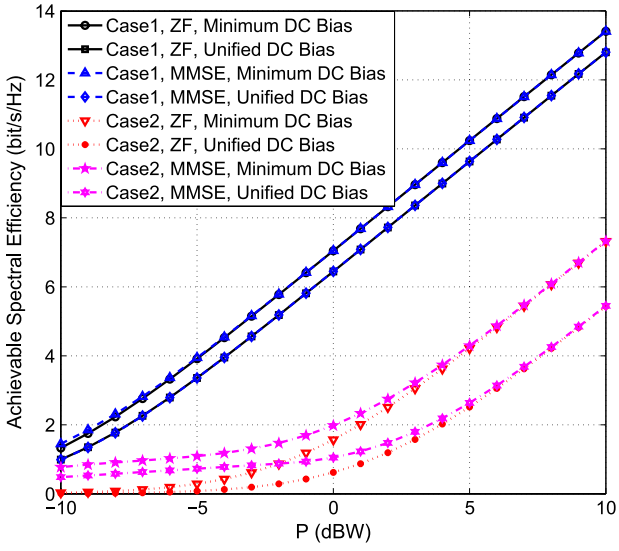

Fig. 4. Average spectral efficiency with different average emitted optical power and DC bias.

forcing precoding is employed. It can be seen that ACO-OFDM-based schemes outperforms DCO-OFDM-based schemes when the emitted optical power is low for both cases. When the emitted optical power increases and the achievable spectral efficiency is above 6 bits/s/Hz, however, the performance of ACO-OFDM-based scheme is even worse. The reason is, although the disuse of DC bias in ACO-OFDM can improve the power efficiency and thus supporting higher-order modulations with the same optical power, half of the subcarriers are wasted. The benefits provided by power decrease can not make up the loss in spectral efficiency when high-order modulations are used, which matches our analysis in Section 3.3.

5. Conclusion

In this paper, MU-MIMO-OFDM is studied for VLC systems, which considers the phase differences of channel matrices in the frequency domain induced by the distance differences of the multiple transmitter-receiver links. Different from state-of-the-art MU-MIMO VLC schemes, zero

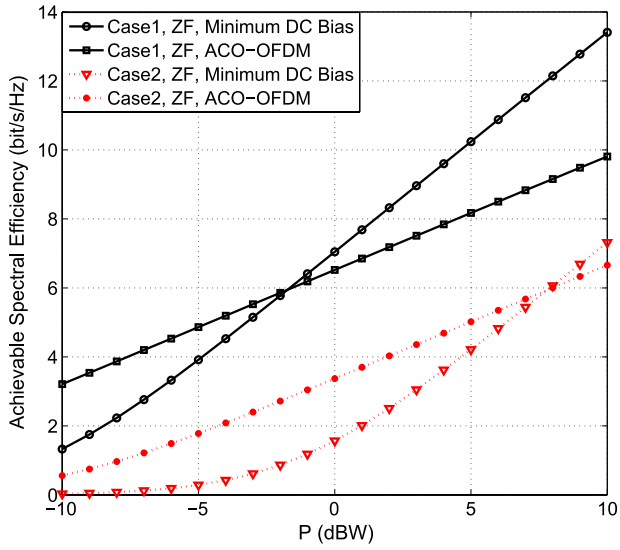

Fig. 5. Average spectral efficiency comparison of ACO-OFDM-based and DCO-OFDM-based schemes with different average emitted optical power.

forcing and MMSE precoding techniques are performed on the complex channel matrices for each subcarrier, which are less correlated when the phase differences are considered. Minimum DC bias, unified DC bias, and ACO-OFDM-based scheme are proposed for different sceneries to achieve intensity modulation. Simulation results illustrate that the subcarrier with higher index achieves more spectral efficiency, especially when the users are highly correlated. MMSE precoding outperforms that with zero forcing when the optical power is low and when more performance gain is achieved when the users are closer.

References

[1] R. Zhang *et al.,* "Visible light communications in heterogeneous networks: Pave the way for user-centric design," *IEEE Wireless Commun.*, vol. 22, no. 2, pp. 8–16, Apr. 2015.
[2] Q. Gao, C. Gong, S. Li, and Z. Xu, "DD-informative modulation for visible light communications under lighting constraints," *IEEE Wireless Commun.*, vol. 22, no. 2, pp. 54–60, Apr. 2015.
[3] F. Haider *et al.,* "Cellular architecture and key technologies for 5G wireless communication networks," *IEEE Commun. Mag.*, vol. 52, no. 2, pp. 122–130, Feb. 2014.
[4] S. Wu, H. Wang, and C. Youn, "Visible light communications for 5G wireless networking systems: From fixed to mobile communications," *IEEE Netw.*, vol. 28, no. 6, pp. 41–45, Nov./Dec. 2014.
[5] J. Grubor, S. C. J. Lee, K.-D. Langer, T. Koonen, and J. W. Walewski, "Wireless high-speed data transmission with phosphorescent white-light LEDs," in *Proc. ECOC*, 2007, pp. 1–2.
[6] J. Ding, Z. Xu, and L. Hanzo, "Accuracy of the point-source model of a multi-LED array in high-speed visible light communication channel characterization," *IEEE Photon. J.*, vol. 7, no. 4, Aug. 2015, Art. ID 1600714.
[7] T. Fath and H. Haas, "Performance comparison of MIMO techniques for optical wireless communications in indoor environments," *IEEE Trans. Commun.*, vol. 61, no. 2, pp. 733–742, Feb. 2013.
[8] Z. Yu, R. J. Baxley, and G. T. Zhou, "Multi-user MISO broadcasting for indoor visible light communication," in *Proc. IEEE ICASSP*, Vancouver, BC, Canada, May 2013, pp. 4849–4853.
[9] H. Ma, L. Lampe, and S. Hranilovic, "Robust MMSE linear precoding for visible light communication broadcasting systems," in *Proc. IEEE Globecom Workshops*, Atlanta, GA, USA, Dec. 2013, pp. 1081–1086.
[10] Y. Hong, J. Chen, Z. Wang, and C. Yu, "Performance of a precoding MIMO system for decentralized multiuser indoor visible light communications," *IEEE Photon. J.*, vol. 5, no. 4, Aug. 2013, Art. ID 7800211.
[11] B. Li *et al.,* "Multiuser MISO transceiver design for indoor downlink visible light communication under per-LED optical power constraints," *IEEE Photon. J.*, vol. 7, no. 4, Aug. 2015, Art. ID 7201415.
[12] L. Zeng *et al.,* "High data rate Multiple Input Multiple Output (MIMO) optical wireless communications using white LED lighting," *IEEE J. Sel. Areas Commun.*, vol. 27, no. 9, pp. 1654–1662, Dec. 2009.
[13] G. Cossu, A. M. Khalid, P. Choudhury, R. Corsini, and E. Ciaramella, "3.4 Gbit/s visible optical wireless transmission based on RGB LED," *Opt. Exp.*, vol. 20, no. 26, pp. B501–B506, Dec. 2012.
[14] W. Xu, M. Wu, H. Zhang, X. You, and C. Zhao, "ACO-OFDM-specified recoverable upper clipping with efficient detection for optical wireless communications," *IEEE Photon. J.*, vol. 6, no. 5, Oct. 2014, Art. ID 7902617.

[15] Q. Wang, Z. Wang, and L. Dai, "Iterative receiver for hybrid asymmetrically clipped optical OFDM," *J. Lightw. Technol.*, vol. 32, no. 22, pp. 3869–3875, Nov. 2014.
[16] Q. Wang *et al.,* "Layered ACO-OFDM for intensity-modulated direct-detection optical wireless transmission," *Opt. Exp.*, vol. 23, no. 9, pp. 12382–12393, May 2015.
[17] Q. Wang, Z. Wang, and L. Dai, "Asymmetrical hybrid optical OFDM for visible light communications with dimming control," *IEEE Photon. Technol. Lett.*, vol. 27, no. 9, pp. 974–977, May 2015.
[18] G. L. Stuber *et al.,* "Broadband MIMO-OFDM wireless communications," *Proc. IEEE*, vol. 92, no. 2, pp. 271–294, Feb. 2004.
[19] M. Jiang and L. Hanzo, "Multiuser MIMO-OFDM for next-generation wireless systems," *Proc. IEEE*, vol. 95, no. 7, pp. 1430–1469, Jul. 2007.
[20] A. H. Azhar, T. Tran, and D. O'Brien, "A gigabit/s indoor wireless transmission using MIMO-OFDM visible-light communications," *IEEE Photon. Technol. Lett.*, vol. 25, no. 2, pp. 171–174, Jan. 2013.
[21] A. C. Boucouvalas, K. Yiannopoulos, and Z. Ghassemlooy, "100 Gbit/s optical wireless communication system link throughput," *Electron. Lett.*, vol. 50, no. 17, pp. 1220–1222, Aug. 2014.
[22] D. Tsonev, S. Videv, and H. Haas, "Towards a 100 Gb/s visible light wireless access network," *Opt. Exp.*, vol. 23, no. 2, pp. 1627–1637, Jan. 2015.
[23] A. Gomez *et al.,* "Beyond 100-Gb/s indoor wide field-of-view optical wireless communications," *IEEE Photon. Technol. Lett.*, vol. 27, no. 4, pp. 367–370, Feb. 2015.
[24] Q. H. Spencer, A. L. Swindlehurst, and M. Haardt, "Zero-forcing methods for downlink spatial multiplexing in multiuser MIMO channels," *IEEE Trans. Signal Process.*, vol. 52, no. 2, pp. 461–471, Feb. 2004.
[25] Q. H. Spencer, C. B. Peel, A. L. Swindlehurst, and M. Haardt, "An introduction to the multi-user MIMO downlink," *IEEE Commun. Mag.*, vol. 42, no. 10, pp. 60–67, Oct. 2004.
[26] S. D. Dissanayake and J. Armstrong, "Comparison of ACO-OFDM, DCO-OFDM and ADO-OFDM in IM/DD systems," *J. Lightw. Technol.*, vol. 31, no. 7, pp. 1063–1072, Apr. 2013.
[27] J. Armstrong and A. J. Lowery, "Power efficient optical OFDM," *Electron. Lett.*, vol. 42, no. 6, pp. 370–372, Mar. 2006.